Calculation of Phase Trajectories for Microstructural Analysis in Liquidus Fields of Cristobalite and Tridymite for System FeO-SiO$_2$-Fe$_2$O$_3$

V Lutsyk[1,2]**, A Zelenaya**[1] **and M Lamueva**[1]

[1]Institute of Physical Materials Science (Siberian Branch of Russian Academy of Sciences), Ulan-Ude, Russia

[2]Buryat State University, Ulan-Ude, Russia

E-mail: vluts@ipms.bscnet.ru

Abstract. Two spatial models of the phase diagram (PD) of system FeO-SiO$_2$-Fe$_2$O$_3$ have been developed based on the method of computer assembly from phase regions. The first variant presents the simplified phase diagram for system FeO-SiO$_2$-Fe$_2$O$_3$ without taking into account the immiscibility surface and without separation of tridymite field on the liquidus of silicon dioxide. Such model includes five liquidus surfaces corresponding to the initial components and two binary compounds fayalite and magnetite. The second model is more accurate and takes into account the presence of a two-phase region of liquid immiscibility, which divides the cristobalite field into two parts. It includes eight liquidus surfaces: two parts of cristobalite, iron, hematite, tridymite, fayalite, wustite, magnetite. The liquidus field of Fe is hypothetical. The surfaces of solidus, solvus, ruled surfaces are constructed and the phase regions are formed. Based on the complete computer model, the possibility of microstructural composition analyzes for system FeO-SiO$_2$-Fe$_2$O$_3$ in the crystallization fields of cristobalite and tridimite is demonstrated using the diagrams of vertical mass balance, calculated for a given mass center in all temperature range of crystallization. Two-, one-, and zero-dimensional concentration fields with coincided and individual sets of micro-constituents are shown.

1. Introduction

The system FeO-Fe$_2$O$_3$-SiO$_2$ is of great practical significance and it is important in the description of pyrometallurgical processes, in the production of ceramics and refractories, and also in the description of petrological processes.

For a more accurate understanding of the occurring physico-chemical processes, computer models of phase diagrams (PD) become an effective tool for analyzing the phase trajectories and micro-constituents.

The difficulty of studying of system FeO-SiO$_2$-Fe$_2$O$_3$ consists in the fact that an accurate (specific) description both the bounding systems FeO-SiO$_2$ and FeO-Fe$_2$O$_3$, and the liquidus surfaces isn't yet given. The regions of liquid immiscibility are also given fragmentarily.

As for the system FeO-SiO$_2$, it is noted that at a high FeO content there is a small amount of Fe$_2$O$_3$ and therefore the system is not strictly binary one [1]. An approximate PD is given for it with immiscible melts region near SiO$_2$, two binary eutectic points and the compound fayalite (Fe$_2$SiO$_4$) with congruent melting [1-3].

The binary system FeO-Fe$_2$O$_3$ is presented as part of system Fe-O with three compounds taken into account: wustite (FeO) – with incongruent melting, magnetite (Fe$_3$O$_4$) and hematite (Fe$_2$O$_3$) -

with congruent melting [1-2, 4-5]. PD of subsystem $FeO–Fe_2O_3$ includes the fragments of liquids immiscibility region and two-phase regions with Fe, which further complicate the ternary system in consideration.

For the SiO_2-Fe_2O_3 binary system, an approximate PD is given, which is characterized by the large region of the melts immiscibility and one eutectic point [1].

On PD of ternary system FeO-SiO_2-Fe_2O_3 (A–B–C) [1-2, 6–7], the liquidus fields corresponding to the wustite FeO and fayalite (Fe_2SiO_4) do not adjoin the bounding system $FeO–SiO_2$.

Since the system $FeO–Fe_2O_3$ contains fragments of phase regions with Fe and corresponding immiscibility region, the liquidus surface Fe and the adjacent immiscibility surface are partially presented for the ternary system. The liquidus surfaces Fe_2O_3, SiO_2, tridimite, cristobalite, and the immiscibility surface near the SiO_2 component, which occupies most of the diagram, are also partially shown.

So, the system FeO-SiO_2-Fe_2O_3 (A-B-C) contains eight liquidus fields (Fe, SiO_2, Fe_2O_3, SiO_2^{cr}, SiO_2^{tr}, Fe_2SiO_4, FeO, Fe_3O_4), immiscibility surface and four invariant points. PD with a similar topology was also obtained as a result of thermodynamic calculations [8].

V.A. Zharikov [9] proposed a schematic model of PD for system FeO-SiO_2-Fe_2O_3, without the region of liquids immiscibility and SiO_2 polymorphism. Such PD prototype is the initial stage in the development of a computer model.

The development of three-dimensional computer models based on assemblies from phase regions makes it possible to take into account the different variants of topological structures for studied PD. The obtained models can be supplemented and changed with the appearance of new data regarding the topological structure of PD.

The experimental information about bounding binary systems and primary crystallization surfaces, taking into account the melting type of binary compounds are used as initial data for construction of computer models. Namely, the coordinates and temperatures of points on the surfaces contour, the curvature of surfaces ware taken into account.

A spatial scheme of mono- and invariant states of system FeO-SiO_2-Fe_2O_3 is developed based on these data. The scheme not only includes a list of mono- and invariant reactions, but also describes the contour of ruled surfaces at the boundary of phase regions. Such scheme determines the arrangement of horizontal complexes at temperatures of invariant points, and then the ruled surfaces are added at the boundary of three-phase regions. Step by step reconstruction of the phase regions boundaries allows us to obtain the complete PD model of studied system [10–11].

The kinematic method was used for describing the liquidus surfaces and ruled surfaces on the boundaries of three-phase regions [12–13].

The computer model of PD is a tool for its comprehensive study. Model makes it possible to obtain data on the stages of crystallization process and the formation of microstructural elements as well as the calculation of horizontal and vertical section [14-15].

2. The prototype of PD for system FeO-SiO_2-Fe_2O_3 (A-B-C) according to V.A. Zharikov [8]

The simplified PD includes five liquidus surfaces, corresponding to the initial components FeO (wustite), SiO_2, Fe_2O_3 (hematite) and two binary compounds fayalite ($R_1=Fe_2SiO_4$) and magnetite ($R_2=Fe_3O_4$). It is assumed, that three eutectic invariant transformations $L_{E1}{\rightarrow}A+R_1+R_2$, $L_{E2}{\rightarrow}B+R_1+R_2$, $L_{E3}{\rightarrow}B+C+R_2$ take place in the system (Scheme 1). On the monovariant liquidus curves there are two Van Rijn points: e_1 on the line E_1E_2 and e_2 on the line E_2E_3.

To simplify, the model is constructed without taking into account the solid-phase solubility. It is assumed that the surfaces of solidus and solvus, as well as the ruled surfaces associated with them, are degenerated on the edges and faces of prism, and both binary compounds have a constant composition. As a result, a simplified model of system FeO-SiO_2-Fe_2O_3 is formed by 5 liquidus surfaces, 20 ruled surfaces at the boundaries of two- and three-phase regions, 3 horizontal complexes at invariant points temperatures; contains 7 two-phase regions and 10 three-phase regions (Tables 1-2, Figure 1).

Scheme 1. Scheme of mono- and invariant states of system FeO-SiO_2-Fe_2O_3 (A-B-C) with temperature range
$C(Fe_2O_3) > B(SiO_2) > e_{BC} > R_2 > e_{CR2} > e_2 > E_3 > A(FeO) > e_{AR2} > R_1 > e_{BR1} > e_{AR1} > e_1 > E_1 > E_2$.

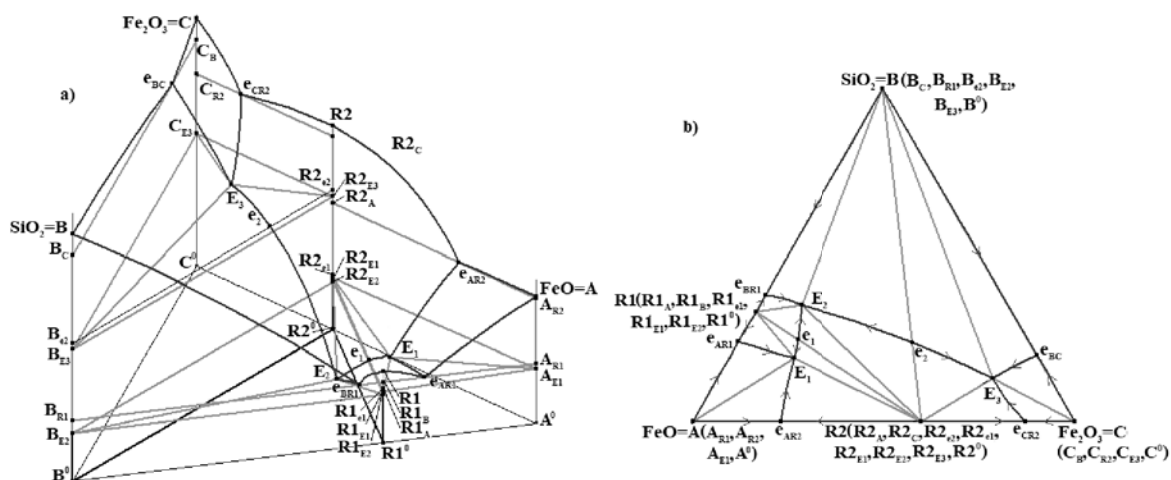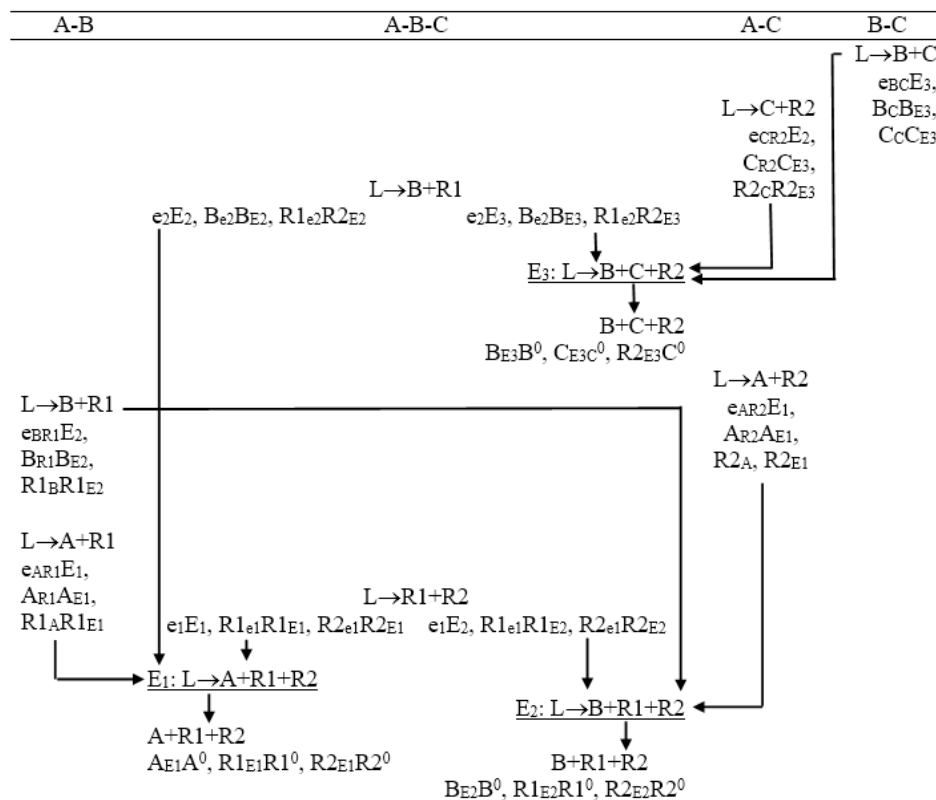| A-B	A-B-C	A-C	B-C

$L \to B+C$
$e_{BC}E_3,$
$B_CB_{E3},$
C_CC_{E3}

$L \to C+R2$
$e_{CR2}E_2,$
$C_{R2}C_{E3},$
$R2_CR2_{E3}$

$L \to B+R1$
$e_2E_2, B_{e2}B_{E2}, R1_{e2}R2_{E2}$

$e_2E_3, B_{e2}B_{E3}, R1_{e2}R2_{E3}$

$\underline{E_3: L \to B+C+R2}$

$B+C+R2$
$B_{E3}B^0, C_{E3}C^0, R2_{E3}C^0$

$L \to A+R2$
$e_{AR2}E_1,$
$AR2_{AE1},$
$R2_A, R2_{E1}$

$L \to B+R1$
$e_{BR1}E_2,$
$B_{R1}B_{E2},$
$R1_BR1_{E2}$

$L \to A+R1$
$e_{AR1}E_1,$
$AR1_{AE1},$
$R1_AR1_{E1}$

$L \to R1+R2$
$e_1E_1, R1_{e1}R1_{E1}, R2_{e1}R2_{E1}$ $e_1E_2, R1_{e1}R1_{E2}, R2_{e1}R2_{E2}$

$\underline{E_1: L \to A+R1+R2}$

$A+R1+R2$
$A_{E1}A^0, R1_{E1}R1^0, R2_{E1}R2^0$

$\underline{E_2: L \to B+R1+R2}$

$B+R1+R2$
$B_{E2}B^0, R1_{E2}R1^0, R2_{E2}R2^0$

Figure 1. 3D model (a) and XY projection of PD for system FeO-SiO_2-Fe_2O_3 (A-B-C) (b) by [8]

Table 1. Surfaces contours.

Name	Contour	Name	Contour
		Liquidus	
q_A	$Ae_{AR1}E_1e_{AR2}$	q_{R1}	$e_{AR1}R1e_{BR1}E_2e_1E_1$

q_B	$Be_{BR1}E_2e_2E_3e_{BC}$	q_{R2}	$e_{AR2}E_1e_1E_2e_2E_3e_{CR2}R2$
q_C	$Ce_{CR2}E_3e_{BC}$		

Ruled surfaces

q^r_{AR1}	$e_{AR1}E_1A_{E1}A_{R1}$	q^r_{CR2}	$e_{CR2}E_3C_{E3}C_{R2}$
q^r_{R1A}	$e_{AR1}E_1R1_{E1}R1_A$	q^r_{R2C}	$e_{CR2}E_3R2_{E3}R2_C$
q^r_{AR2}	$e_{AR2}E_1A_{E1}A_{R2}$	q^r_{R1R2}	$E_1e_1E_2R1_{E2}R1_{e1}R1_{E1}$
q^r_{R2A}	$e_{AR2}E_1R2_{E1}R2_A$	q^r_{R2R1}	$E_1e_1E_2R2_{E2}R2_{e1}R2_{E1}$
q^r_{BR1}	$e_{BR1}E_2B_{E2}B_{R1}$	s^r_{R1R2}	$R1_{E1}R1_{E2}R2_{E2}R2_{E1}$
q^r_{R1B}	$e_{BR1}E_2R1_{E2}R1_B$	s^r_{BR2}	$B_{E2}B_{E3}R2_{E3}R2_{E2}$
q^r_{BR2}	$E_2e_2E_3B_{E3}B_{e2}B_{E2}$	v^r_{R1R2}	$R1_{E1}R2_{E1}R2^0R1^0$
q^r_{R2B}	$E_2e_2E_3R2_{E3}R2_{e2}R2_{E2}$	v^r_{R2R1}	$R1_{E2}R2_{E2}R2^0R1^0$
q^r_{BC}	$e_{BC}E_3B_{E3}B_C$	v^r_{BR2}	$B_{E2}R2_{E2}R2^0B^0$
q^r_{CB}	$e_{BC}E_3C_{E3}C_B$	v^r_{R2B}	$B_{E3}R2_{E3}R2^0B^0$

Horizontal complexes

h^{E1}	h^{E1}_{AR1E1}	$A_{E1}R1_{E1}E_1$	h^{E2}	h^{E2}_{BR1E2}	$B_{E2}R1_{E2}E_2$	h^{E3}	h^{E3}_{BCE3} $B_{E3}C_{E3}E_3$
	h^{E1}_{AR2E1}	$A_{E1}R2_{E1}E_1$		h^{E2}_{BR2E2}	$B_{E2}R2_{E2}E_2$		h^{E3}_{BR2E3} $B_{E3}R2_{E3}E_3$
	h^{E1}_{R1R2E1}	$R1_{E1}R2_{E1}E_1$		h^{E2}_{R1R2E2}	$R1_{E2}R2_{E2}E_2$		h^{E3}_{CR2E3} $C_{E3}R2_{E3}E_3$
	h^{E1}_{AR1R1}	$A_{E1}R1_{E1}R2_E$		h^{E2}_{BR1R2}	$B_{E2}R1_{E2}R2_{E2}$		h^{E3}_{BCR2} $B_{E3}C_{E3}R2_{E3}$

Table 2. Structure of phase regions.

Phase region	Boundary surfaces	Phase region	Boundary surfaces
L+A	$q_A, q^r_{AR1}, q^r_{AR2}$	**L+B+C**	$q^r_{BC}, q^r_{BC}, h^{E3}_{BCE3}$
L+B	$q_B, q^r_{BR1}, q^r_{BR2}, q^r_{BC}$	**L+C+R2**	$q^r_{CR2}, q^r_{R2C}, h^{E3}_{CR2E3}$
L+C	q_C, q^r_{CB}, q^r_{CR2}	**L+R1+R2**	$q^r_{R1R2}, q^r_{R2R1}, s^r_{R1R2}, h^{E1}_{R1R2E1},$ h^{E2}_{R1R2E2}
L+R1	$q_{R1}, q^r_{R1A}, q^r_{R1R2}, q^r_{R1B}$	**R1+R2**	$s^r_{R1R2}, v^r_{R1R2}, v^r_{R2R1}$
L+R2	$q_{R2}, q^r_{R2A}, q^r_{R2R1}, q^r_{R2B}, q^r_{R2C}$	**B+R2**	$s^r_{BR2}, v^r_{BR2}, v^r_{R2B}$
L+A+R1	$q^r_{AR1}, q^r_{R1A}, h^{E1}_{AR1E1}$	**A+R1+R2**	$h^{E1}_{AR1R2}, v^r_{R1R2}$
L+A+R2	$q^r_{AR2}, q^r_{R2A}, h^{E1}_{AR2E1}$	**B+R1+R2**	$h^{E2}_{BR1R2}, v^r_{R2R1}, v^r_{BR2}$
L+B+R1	$q^r_{BR1}, q^r_{R1B}, h^{E2}_{BR1E2}$	**B+C+R2**	h^{E3}_{BCR2}, v^r_{R2B}
L+B+R2	$q^r_{BR2}, q^r_{R2B}, s^r_{BR2}, h^{E2}_{BR2E2},$ h^{E3}_{BR2E3}		

3. Complete model of PD for system FeO-SiO$_2$-Fe$_2$O$_3$ (A-B-C)

The simplified model is the basis (template) for constructing the more complete PD model, taking into account the features of the topological structure of system FeO-SiO$_2$-Fe$_2$O$_3$. The system FeO-SiO$_2$-Fe$_2$O$_3$ (A-B-C) contains eight liquidus fields (Fe, Fe$_2$O$_3$, two fields of cristobalite=B1, tridimite =B2, 2FeO·SiO$_2$=R$_1$, FeO=R$_2$, FeO·Fe$_2$O$_3$=R$_3$) and immiscibility surface. There are four invariant transformations: three eutectics (L$_{E1}$→R$_1$+R$_2$+R$_3$, L$_{E2}$→B+R$_1$+R$_3$, L$_{E3}$→B+C+R$_3$) and one metatectic, corresponding to the transition from a high-temperature polymorphic modification of silica (B1 - cristobalite) to low-temperature modification (B2 – tridymite) (B$_1$→L$_V$+B$_2$+C). The cristobalite field is divided by the immiscibility surface into two fragments Bm$_1$m$_2$ and n$_1$n$_2$e$_{B1C}$Vk$_{BR1}$.

The model was constructed taking into account the presence of Fe; therefore, the liquidus surface Fe was given, but the adjacent to it a immiscibility surface was not considered. Since the system FeO-SiO$_2$ (A-B) is not strictly binary, the surfaces are formed in such way that they do not touch the corresponding face of prism near the vertex A. In particular binary points e$_{BR1}$, e$_{AR1}$, e$_{BR2}$, R1 do not adjoin the bounding system A-B. The region of liquids immiscibility occupies a wide area.

Compounds R$_2$ and R$_3$ have the variable composition and therefore corresponding solidus and solvus surfaces were constructed. In other cases, the surfaces of solidus and solvus have a degenerate

structure. So, PD model contains the immiscibility surface near SiO_2 component, 8 liquidus surfaces, 2 solidus, 8 solvus, 35 ruled surfaces, 4 horizontal complexes at the temperatures of invariant point (Figure 2, Table 3). The phase regions are formed: 2 one-phase regions (R2, R3), 13 two-phase regions (L1+L2, L+B, L+B1, L+B2, L+C, L+R1, L+R2, L+R3, R1+R2, R1+R3, R2+R3 B2+R3, C+R3), 13 three-phase regions (L1+L2+B, L+B1+B2, L+B1+C, L+B2+C, L+B2+R1, L+B2+R3, L+R1+R2, L+R1+R3, L+R2+R3, L+C+R3, R1+R2+R3, B2+R1+R3, B2+C+R3) (Table 4).

The monovariant liquidus line $k_{BR1}V$ on the boundary of liquidus surfaces of cristobalite (B1) and tridimite (B2) is located at the same temperature. Points $B1_V$ and $B2_V$ are combined together on the prism edge and therefore the plane corresponding to the metatectic equilibrium (V: $B_1 \rightarrow L_V + B_2 + C$) has a degenerate structure $VC_V B1_V (B2_V)$. Therefore, the phase region L+B1+B2 is degenerated into a plane and the corresponding monovariant peritectic reaction $L^p + B1 \rightarrow B2^p$ proceeds at the same temperature.
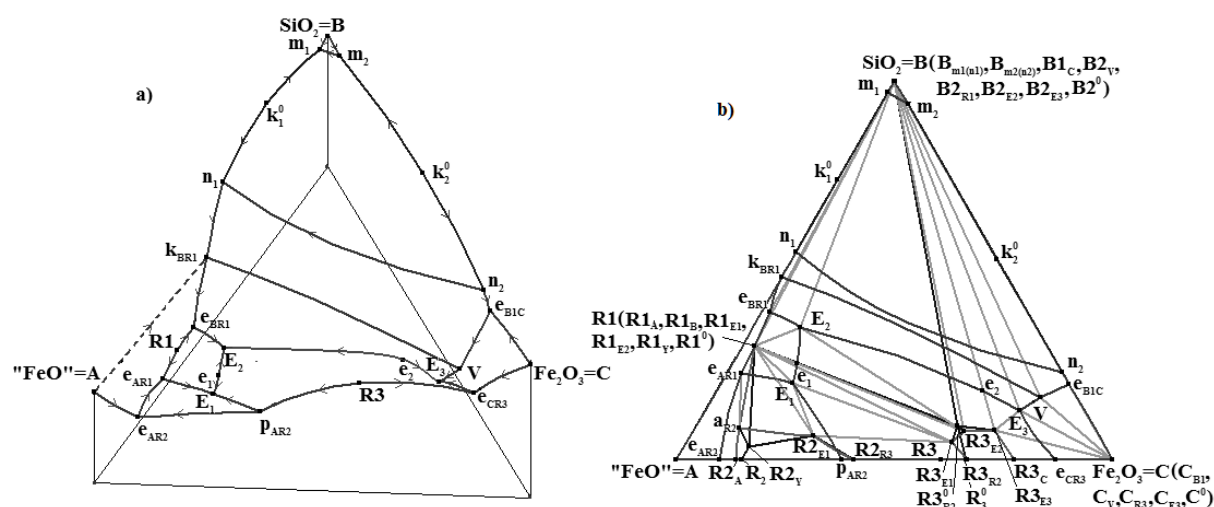

Figure 2. 3D model of immiscibility and liquidus surfaces (a), XY projection of all surfaces of system $FeO-SiO_2-Fe_2O_3$ (A-B-C) (b)

Table 3. Surfaces contours.

Name	Contour	Name	Contour
Liquidus			
q_A	$Ak_{BR1}e_{BR1}R1e_{AR1}e_{AR2}$	q_C	$Ce_{CR3}E_3Ve_{B1C}$
q^u_{B1}	Bm_1m_2	q_{R1}	$e_{AR1}R1e_{BR1}E_2e_1E_1$
q^d_{B1}	$n_1n_2e_{B1C}Vk_{BR1}$	q_{R2}	$e_{AR2}e_{AR1}E_1p_{AR2}$
q_{B2}	$e_{BR1}k_{BR1}VE_3e_2E_2$	q_{R3}	$p_{AR2}E_1e_1E_2e_2E_3e_{CR3}R3$
Immiscibility surface			
$k_1^0m_1m_2k_2^0n_2n_1$			
Solidus			
s_{R2}	$R2_Aa_{R2}R2_{E1}R2_{R3}$	s_{R3}	$R3_{R2}R3_{E1}R3_{E2}R3_{E3}R3_CR3$
Solvus			
v_{R1R2}	$R2_Aa_{R2}R2_YR2$	v_{R3C}	$R3_CR3_{E3}R3^0_{R2}R3^0$
v_{R2R3}	$R2R2_YR2_{E1}R2_{R3}$	v_{R3B2}	$R3_{E2}R3_{E3}R3^0_{R2}$
v_{R2B}	$R2_Ya_{R2}R2_{E1}$	v_{R3R1}	$R3_{E1}R2_{E2}R3^0_{R2}$
v_{R3R2}	$R3_{R2}R3_{E1}R3^0_{R2}R3^0$	v_{R2}	$R2_YR2R2^0$
Ruled surfaces			
i^r	$m_1m_2n_2n_1$	q^r_{CR3}	$e_{CR3}E_3C_{E3}C_{R3}$
i^r_n	$n_1n_2B_{m1(n1)}$	q^r_{R3C}	$e_{CR3}E_3R3_{E3}R3_C$

i^r_m	$m_1 m_2 B_{m1(n1)}$	s^r_{AR2}	$e_{AR2} e_{AR1} a_{R2} R2_A$
q^r_{R1R2}	$e_{AR1} E_1 R1_{E1} R1_A$	s^r_{R1R2}	$a_{R2} R1_A R1_{E1} R2_{E1}$
q^r_{R2R1}	$e_{AR1} E_1 R2_{E1} a_{R2}$	s^r_{R2R3}	$R2_{R3} R2_{E1} R3_{E1} R3_{R2}$
q^r_{R1R3}	$E_1 e_1 E_2 R1_{E2} R1_{e1} R1_{E1}$	s^r_{R1R3}	$R1_{E1} R1_{E2} R3_{E2} R3_{E1}$
q^r_{R3R1}	$E_1 e_1 E_2 R3_{E2} R3_{e1} R3_{E1}$	s^r_{B2R3}	$B2_{E2} B2_{E3} R3_{E3} R3_{E2}$
q^r_{B2R1}	$e_{BR1} E_2 B2_{E2} B2_{R1}$	s^r_{CR3}	$C_{R3} C_{E3} R3_{E3} R3_C$
q^r_{R1B2}	$e_{BR1} E_2 R1_{E2} R1_B$	v^r_{R1R2}	$a_{R2} R2_Y R1_Y R1_A$
q^r_{B2R3}	$E_2 e_2 E_3 B2_{E3} B2_{e2} B2_{E2}$	v^r_{R2R1}	$R1_Y R1_{E1} R2_{E1} R2_Y$
q^r_{R2B2}	$E_2 e_2 E_3 R3_{E3} R3_{e2} R3_{E2}$	v^r_{R1R3}	$R1_{E2} R3_{E2} R3^0_{R2} R1^0$
q^r_{B2C}	$E_3 V B2_V B2_{E3}$	v^r_{R3R1}	$R1_{E1} R3_{E1} R3^0_{R2} R1^0$
q^r_{CB2}	$E_3 V C_V C_{E3}$	v^r_{BR3}	$B2_{E2} R3_{E2} R3^0_{R2} B2^0$
q^r_{B1B2}	$k_{BR1} V B2_V$	v^r_{R3B}	$B2_{E3} R3_{E3} R3^0_{R2} B2^0$
q^r_{B1C}	$e_{B1C} V B2_V B1_C$	$v^r_{R1R2\ 0}$	$R1_Y R2_Y R2^0 R1^0$
q^r_{CB1}	$e_{B1C} V C_V C_{B1}$	v^r_{R2R3}	$R2_{E1} R3_{E1} R3^0_{R2} R2^0$
q^r_{R2R3}	$p_{AR2} E_1 R2_{E1} R2_{R3}$	v^r_{R3C}	$C_{E3} R3_{E3} R3^0_{R2} C^0$
q^r_{R3R2}	$p_{AR2} E_1 R3_{E1} R3_{R2}$		

Horizontal complexes						
h^{E1}	h^{E1}_{R1R2E1}	$R1_{E1} R2_{E1} E_1$	h^{E2}	h^{E2}_{B2R1E2}	$B2_{E2} R1_{E2} E_2$	
	h^{E1}_{R1R3E1}	$R1_{E1} R3_{E1} E_1$		h^{E2}_{B2R3E2}	$B2_{E2} R3_{E2} E_2$	
	h^{E1}_{R2R3E1}	$R2_{E1} R3_{E1} E_1$		h^{E2}_{R1R3E2}	$R1_{E2} R3_{E2} E_2$	
	h^{E1}_{R1R2R3}	$R1_{E1} R2_{E1} R3_{E1}$		h^{E2}_{B2R1R3}	$B2_{E2} R1_{E2} R3_{E2}$	

h^{E3}	h^{E3}_{B2CE3}	$B2_{E3} C_{E3} E_3$
	h^{E3}_{B2R3E3}	$B2_{E3} R3_{E3} E_3$
	h^{E3}_{CR3E3}	$C_{E3} R3_{E3} E_3$
	h^{E3}_{B2CR3}	$B2_{E3} C_{E3} R3_{E3}$

h_V	$V B2_V C_V$

Table 4. Structure of phase regions.

Phase region	Boundary surfaces	Phase region	Boundary surfaces
L1+L2	i, i^r	**L+R1+R2**	q^r_{R1R2}, q^r_{R2R1}, s^r_{R1R2}, h^{E1}_{R1R2E1}
L+R1	q_{R1}, q^r_{R1R2}, q^r_{R1B2}, q^r_{R1R3}	**L+R1+R3**	q^r_{R1R3}, q^r_{R3R1}, s^r_{R1R3}, h^{E1}_{R1R3E1}, h^{E2}_{R1R3E2}
L+R2	q_{R2}, s_{R2}, q^r_{R2R1}, q^r_{R2R3}	**L+R2+R3**	q^r_{R2R3}, q^r_{R3R2}, s^r_{R2R3}, h^{E1}_{R2R3E1}
L+R3	q_{R3}, s_{R3}, q^r_{R3C}, q^r_{R3B2}, q^r_{R3R2}, q^r_{R3R1}	**L+C+R3**	q^r_{CR3}, q^r_{R3C}, s^r_{CR3}, h^{E3}_{CR3E3}
L+B	q^u_{B1}, i^r_m	**R2**	s_{R2}, v_{R2B}, v_{R2R3}, v_{R1R2}
L+B1	q^d_{B1}, q^r_{B1C}, q^r_{B1B2}	**R3**	s_{R3}, v_{R3R1}, v_{R3B2}, v_{R3C}, v_{R3R2}
L+B2	q_{B2}, q^r_{B1B2}, q^r_{B2R1}, q^r_{B2R3}, q^r_{B2C}	**R1+R2**	v_{R2B}, s^r_{R1R2}, v^r_{R1R2}, v^r_{R2R1}
L+C	q_C, q^r_{CB1}, q^r_{CB2}, q^r_{CR3}	**R1+R3**	v_{R3R1}, s^r_{R1R3}, v^r_{R1R3}, v^r_{R3R1}
L1+L2+B	i^r, i^r_m, i^r_n	**B+R2**	v_{R3B2}, s^r_{B2R3}, v^r_{B2R3}, v^r_{R3B2}
L+B1+B2	q^r_{B1B2}	**R2+R3**	v_{R2}, v_{R2R3}, v_{R3R2}, s^r_{R2R3}, v^r_{R2R3}
L+B1+C	q^r_{B1C}, q^r_{CB1}, h_V	**R3+C**	v_{R3C}, s^r_{CR3}, v^r_{R3C}
L+B2+C	q^r_{B2C}, q^r_{CB2}, h_V, h^{E3}_{B2CE3}	**R1+R2+R3**	h^{E1}_{AR1R2}, v^r_{R2R1}, $v^r_{R1R2\_0}$, v^r_{R2R3}, v^r_{R3R1}
L+B2+R1	q^r_{B2R1}, q^r_{R1B2}, h^{E2}_{B2R1E2}	**B2+R1+R3**	h^{E2}_{B2R1R3}, v^r_{R1R3}, v^r_{B2R3}
L+B2+R3	q^r_{B2R3}, q^r_{R3B2}, s^r_{B2R3}, h^{E2}_{B2R3E2}, h^{E3}_{B2R3E3}	**B2+C+R3**	h^{E3}_{B2CR3}, v^r_{R3C}, v^r_{R3B2}

4. Microstructural analysis in the liquidus fields of cristobalite and tridymite

Based on a computer model the triangle of compositions is divided into concentration fields by projecting all elements on the base of trigonal prism. Crystallization stages are compiled and the microstructural composition is established for each concentration field. This is analytically confirmed by vertical material balance diagrams calculated for a given mass center over all temperature range. At

that the quantitative ratios are calculated not only each of the coexisting phases, but also the porions of their microstructural constituents as well [14-15].

Let's consider this technology for the liquidus fields of cristabolite and tridymite.

The crystallization fields of cristobalite (Bm_1m_2, $n_1n_2e_{B1C}Vk_{BR1}$) and tridimite ($e_{BR1}k_{BR1}VE_3e_2E_2$) are divided into 26 two-dimensional fields, 50 one-dimensional fields and 29 zero-dimensional fields (Figure 3).
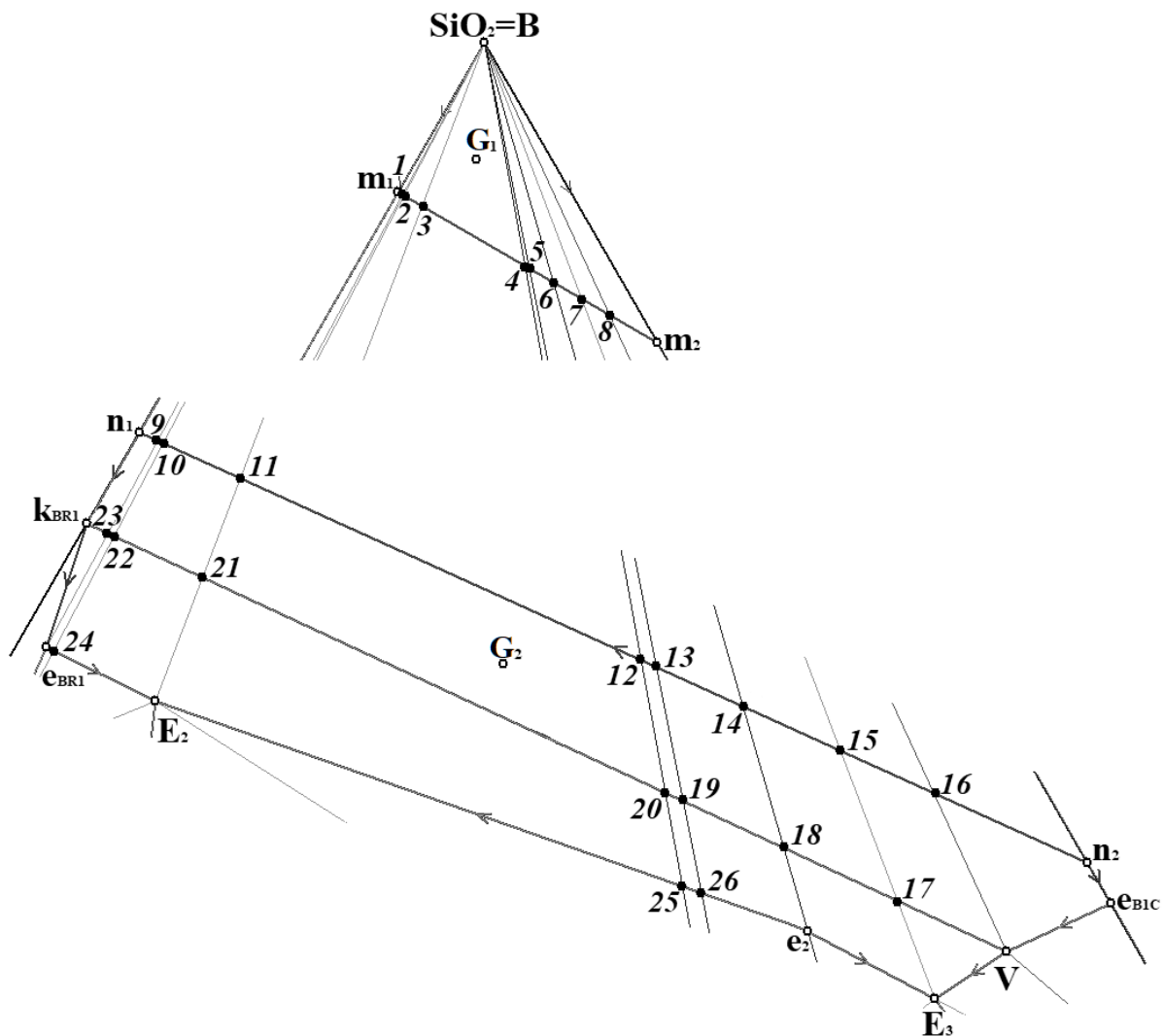

Figure 3. PD fragment with dividing of cristobalite and tridymite liquiduses into concentration fields

The liquidus surface of cristobalite is divided into two parts by the immiscibility surface.

The processes taking place in the phase regions L+B1 and L1+L2+B1 do not affect the final set of micro-constituents, because the products of the reactions occurring there are completely consumed. Therefore, the corresponding two-dimensional fields of cristobalite separated by the immiscibility region have the same micro-constituents, although they differ in crystallization stages.

So, a monovariant monotectic reaction $L_1^m \rightarrow L_2^m + B_1^m$ corresponding to the phase region L1+L2+B1 will additionally occurs in all two-dimensional fields adjacent to the vertex B and in one-dimensional fields located on the line m_1m_2. But all crystals B_1 are consumed during the peritectic reaction $L^p + B_1 \rightarrow B_2^p$, and they do not affect the final set of micro-constituents.

By this means, there are 9 pairs of two-dimensional fields located on both sides of the immiscibility region $m_1m_2n_2n_1$, and 9 corresponding pairs of one-dimensional fields are arranged on lines m_1m_2 and n_1n_2, which have the same micro-constituents, but differ the crystallization stages: $(m_1\text{-B-1})=(n_1\text{-}9\text{-}23\text{-}k_{BR1})=(m_1\text{-}1)=(n_1\text{-}9)$, $(1\text{-B-}2)=(9\text{-}10\text{-}22\text{-}23)=(1\text{-}2)=(9\text{-}10)$, $(2\text{-B-}3)=(10\text{-}11\text{-}21\text{-}22)=(2\text{-}3)=(10\text{-}11)$, $(3\text{-B-}4)=(11\text{-}12\text{-}20\text{-}21)=(3\text{-}4)=(11\text{-}12)$, $(4\text{-B-}5)=(12\text{-}13\text{-}19\text{-}20)=(4\text{-}5)=(12\text{-}13)$, $(5\text{-B-}6)=(13\text{-}14\text{-}18\text{-}19)=(5\text{-}6)=(13\text{-}14)$, $(6\text{-B-}7)=(14\text{-}15\text{-}17\text{-}18)=(6\text{-}7)=(14\text{-}15)$, $(7\text{-B-}8)=(15\text{-}16\text{-V-}17)=(7\text{-}8)=(15\text{-}16)$, $(8\text{-B-}m_2)=(16\text{-}n_2\text{-}e_{B1C}\text{-V})=(8\text{-}m_2)=(16\text{-}n_2)=(e_{B1C}\text{-V})$.

Also, 9 zero-dimensional fields were revealed that coincided in micro-constituents and crystallization stages with neighboring one-dimensional fields: $12=(12\text{-}20)$, $13=(13\text{-}19)$, $14=(14\text{-}18)$, $15=(15\text{-}17)$, $16=(16\text{-V})$, $17=(17\text{-}E_3)$, $19=(19\text{-}26)$, $20=(20\text{-}25)$, $21=(20\text{-}25)$. And eight one-dimensional fields on the line $k_{BR1}V$ coincide with adjacent two-dimensional fields: $(V\text{-}17)=(17\text{-V-}E_3)$, $(17\text{-}18)=(18\text{-}17\text{-}E_3\text{-}e_2)$, $(18\text{-}19)=(19\text{-}18\text{-}e_2\text{-}26)$, $(19\text{-}20)=(20\text{-}19\text{-}26\text{-}25)$, $(20\text{-}21)=(21\text{-}20\text{-}25\text{-}E_2)$, $(21\text{-}22)=(22\text{-}21\text{-}E_2\text{-}24)$, $(22\text{-}23)=(23\text{-}22\text{-}24\text{-}e_{BR1})$, $(23\text{-}k_{BR1})=(k_{BR1}\text{-}e_{BR1}\text{-}23)$.

Let's consider as an example two two-dimensional fields of cristobalite 3-B-4 and 11-12-20-21 (Figure 4). The mass center $G_1(0.014; 0.973; 0.013)$ given in the two-dimensional field 3-B-4 intersects 6 phase regions: L1+B1, L1+L2+B1, (L2+B1), L+B1+B2, L+B2, L+B2+R3, B2+R1+R3.
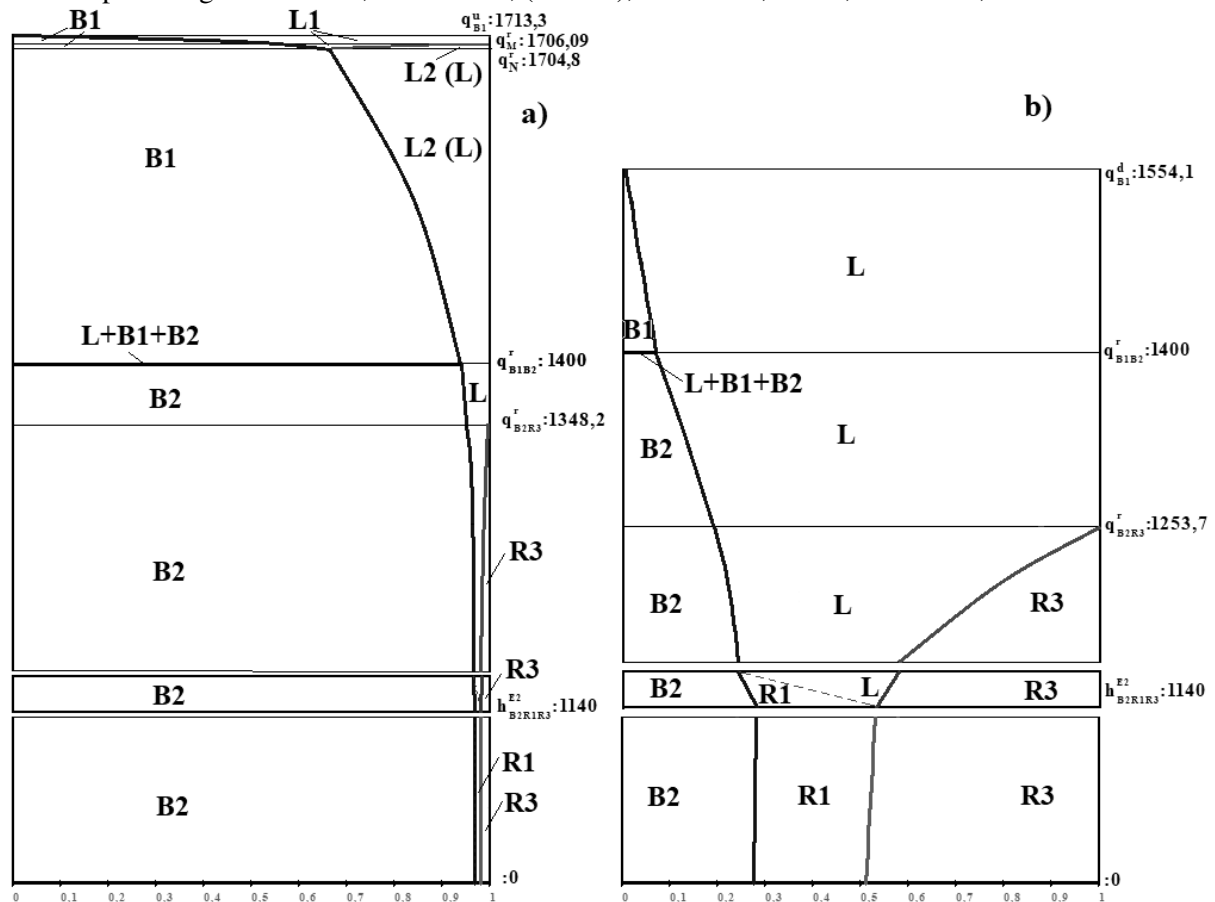

Figure 4. Diagrams of vertical mass balance for mass centers $G_1 \in$ 3-B-4 (a) and $G_2 \in$ 11-12-20-21 (b)

In this case, the mass center twice intersects the phase region L+B1, because it is divided into two fragments by the three-phase region L1+L2+B1. The three-phase region L+B1+B2 has a degenerate structure. As can be seen from the diagram of vertical mass balance (Fig. 4,a), this field is characterized by the following set of phase transformations: $L_1^1 \rightarrow B_1^1$, $L_1^m \rightarrow L_2^m + B_1^m$, $L_2^1 \rightarrow B_1^1$, $L^p + B_1 \rightarrow B_2^p$, $L^{1p} \rightarrow B_2^{1p}$, $L^{ep} \rightarrow B_2^{R3,ep} + R_3^{B2,ep}$, $L^{E2} \rightarrow B_2^{E2} + R_1^{E2} + R_3^{E2}$. As a result, the micro-

constituents is formed: B_2^p, B_2^{1p}, $B_2^{R3,ep}$, $R_3^{B2,ep}$, B_2^{E2}, R_1^{E2}, R_3^{E2}. The crystals B_1 are consumed during the peritectic reaction and are not included in the micro-constituents sets.

The mass center $G_2(0.31; 0.39; 0.3)$ given in the field 11-12-20-21 has a shorter list of phase transformations, because it does not intersect the three-phase region L1+L2+B1 and, accordingly, it intersects once the phase region L+B1: $L^1 \rightarrow B_1^1$, $L^p + B_1 \rightarrow B_2^p$, $L^{1p} \rightarrow B_2^{1p}$, $L^{ep} \rightarrow B_2^{R3,ep} + R_3^{B2,en}$, $L^{E2} \rightarrow B_2^{E2} + R_1^{E2} + R_3^{E2}$.

Thus, the mass centers G_1 and G_2 have the same micro-constituents, but differ in the crystallization stages.

5. Summary

The assembly of 3D model of phase diagram is the final stage of its study by the methods of thermal analysis and X-ray diffraction, and the correction of curvature of curves and surfaces in agreement with the thermodynamic parameters of components and new compounds. If there is the contradictory data, then different variants of PD are assembled. The PD computer model permits to compile the scheme of equilibrium crystallization in the concentration fields of various dimensions (point, line (curve) fragment and fragment of the concentration triangle plane) formed during orthogonal projection of all PD surfaces. This procedure is the main step in decoding the genotype of a heterogeneous material. The concentration fields with unique sets of micro-constituents are revealed as a result of calculation of the qualitative and quantitative composition of microstructure elements. In this case, a list of concentration fields with micro-constituents, which does not differ from the micro-constituents of neighboring fields of smaller or the same dimension is compiled. Analysis of two variants of FeO-SiO_2-Fe_2O_3 PD showed that the presence of immiscibility surface of two melts does not affect the micro-constituents set of the heterogeneous ceramic materials of this system. In the case of application of the ultrafast cooling technology of initial melt and its heterogeneous states at various stages of crystallization, the final set of formed materials can be significantly expanded.

References

[1]   Berezhnoy A S 1970 *Multicomponent oxide systems* (Kiev: Naukova Dumka) (In Russian)

[2]   Levin E M, Robbins C R and McMurdie H F 1964 *Phase diagrams for ceramists* (Ohio: American. Ceramic Society) (In Russian)

[3]   Zavaritsky A N and Sobolev V S 1961 *Physicochemical fundamentals of petrography of igneous rocks* (Moscow: Gosgeoltekhizlat) (In Russian)

[4]   1964 *Data of Geochemistry. Phase-Equilibrium Relations of the Common Rock-Forming Oxides Except Water* Chapter L, ed G W Morey (Washington: United states government printing office)

[5]   Mezentseva L P, Popova V F, Al'myashev V I, Lomanova N A, Ugolkov V L, Beshta S V, Khabenskii V B and Gusarov V V 2006 *Russ. J. Inorg. Chem.* **51** 118

[6]   Muan A and Osborn E F 1965 *Phase Equilibria Among Oxides in Steelmaking* (Massachusetts: Addison-Wesley Publishing Company, Inc.)

[7]   Muan A 1955 *J. Metals* **9** 965

[8]   Hidayat T, Shishin D, Decterov S A and Jak E 2017 *J. Phase Equilib. Diffus.* **38** 477

[9]   Zharikov V A 2005 *Basis of physical geochemistry* (Moscow: Nauka) (In Russian)

[10]   Lutsyk V and Zelenaya A 2013 *IOP Conf. Ser.: Mater. Sci. Eng.* **47** 012047012049

[11]   Lutsyk V I and Zelenaya A E 2018 *Russ. J. Inorg. Chem.* **63** 966

[12]   Lutsyk V I, Zyryanov A M and Zelenaya A E 2008 *Russ. J. Inorg. Chem.* **53** 794

[13] Lutsyk V I, Zelenaya A E and Zyryanov A M 2008 *Journal of Materials, Methods & Technologies, International Science Publications* **2** 176

[14] Lutsyk V and Zelenaya A 2017 *Journal of Physics: Conference Series* **790** 012020

[15] Lutsyk V I and Zelenaya A E 2018 *Russ. J. Inorg. Chem.* **63** 1087